Methyl Chloride Adsorption on Si(001)−Electronic Structure

M. Preuss,* W. G. Schmidt, and F. Bechstedt

Friedrich-Schiller-Universität Jena, 07743 Jena, Germany

Received: January 23, 2004; In Final Form: March 24, 2004

The adsorption of methyl chloride (CH_3Cl) on Si(001) surfaces is studied using *first-principles* calculations based on gradient-corrected density-functional theory (DFT-GGA) and ultrasoft pseudopotentials. The energetically most favored structure for the adsorption of a single molecule is characterized by the dissociation of methyl chloride into CH_3 and Cl fragments, which bond to the same Si dimer. The plausible interface structures are examined with respect to their band structures, surface dipoles, and charge-transfer characteristics. A remarkable sensitivity of the surface electronic properties with respect to the details of the bonding is found.

1. Introduction

The (001) surface of silicon is the starting point for the fabrication of numerous microelectronic devices. For this reason, Si surface reactions with metals, hydrogen, oxygen, and halogens have been intensively studied in the past.[1] Fueled by recent progress in the development of hybrid organic/inorganic devices, reactions of hydrocarbons with silicon surfaces are currently the subject of intensive research.[2] The microscopic understanding of molecule-covered Si surfaces, however, is still limited. That concerns both the reaction mechanisms and details of the bonding but, in particular, the electronic properties.

Here we study computationally the interaction of methyl chloride with the Si(001) surface. The chemistry of chlorine species on Si(001) is relevant in the context of silicon growth from molecules such as dichlorosilane. Chlorine is also commonly used as an etching species in the processing of Si. The interaction of alkyl species with Si has found interest in the context of silicon carbide film growth.

The CH_3Cl/Si interface has been investigated by electron energy loss spectroscopy, Auger electron spectroscopy, and temperature-programmed desorption, as well as scanning tunneling microscopy (STM).[3−5] From the experiments, it was concluded that methyl chloride adsorbs dissociatively on Si. Recently, the adsorption process has also been investigated computationally. However, cluster calculations by Lee and Kim[5] and pseudopotential calculations by Romero et al.[6] arrived at different results concerning the adsorption energetics and equilibrium bonding configurations. In the present study, we focus in particular on the interplay between surface bonding and surface electronic properties of the energetically most relevant interface geometries.

2. Method

The total-energy and electronic-structure calculations are performed using the Vienna Ab-initio Simulation Package (VASP) implementation[7] of the gradient-corrected (PW91)[8] density-functional theory (DFT).

Although PW91, as well as other gradient approximations,[9] intrinsically does not account for dispersion interactions, it has been successfully applied to physisorbed geometries.[10] However, Kganyago and Ngoepe[11] have demonstrated the failure of GGA in the case of graphite where the interlayer bonding is exclusively mediated by van der Waals contributions. Therefore our results for physisorbed adsorption geometries may be of limited accuracy.

The electron−ion interaction is described by non-norm-conserving ultrasoft pseudopotentials,[12] allowing for the accurate quantum-mechanical treatment of first-row elements with a relatively small basis set. We expand the electronic wave functions into plane waves up to an energy cutoff of 25 Ry, which has been demonstrated to be sufficient in our previous studies on small organic molecules in the gas phase[13] and adsorbed on Si(001).[14,15]

The Si(001) surface is modeled with a periodically repeated slab. The supercell consists of eight atomic layers plus adsorbed molecules and a vacuum region equivalent in thickness to 12 atomic layers. The Si bottom layer is hydrogen-saturated and kept frozen during the structure optimization. All calculations are performed using the $c(4 \times 2)$ surface periodicity with the calculated Si equilibrium lattice constant of 5.4562 Å.

Our calculations employ the *residual minimization method−direct inversion in the iterative subspace* (RMM-DIIS) algorithm[16,17] to minimize the total energy of the system. The molecular and surface atomic structure is considered to be in equilibrium when the Hellmann−Feynman forces are smaller than 10 meV/Å. The Brillouin zone integrations for the surface calculations are carried out with four **k** points in its irreducible part.

3. Results and Discussion

3.1. Adsorption Geometries. Clean Si(001) surfaces reconstruct due to the dimerization of the topmost atoms. The dimers are asymmetric, consisting of an sp^2-like bonded "down" atom, which moves closer to the plane of its three nearest neighbors, and an "up" atom, which moves away from the plane of its neighbors and possesses an s-like dangling bond. The process of rehybridization is accompanied by a charge transfer from the "down" to the "up" atom. The direction of buckling alternates within each dimer row. To reduce the energy due to relaxation of local stress and electrostatics, the buckling in the neighboring dimer rows is such that the Si(001) surface ground state is $c(4 \times 2)$ reconstructed.[1,18] This $c(4 \times 2)$ reconstructed Si(001) surface serves as starting point for our calculations on

* Address correspondence to this author. E-mail: preuss@ifto.physik.uni-jena.de.

10.1021/jp049661z CCC: $27.50
Published on Web 05/14/2004

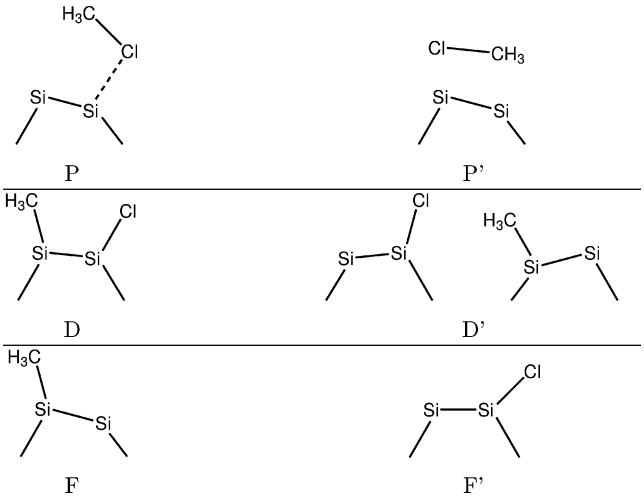

Figure 1. Sketches of the six adsorption geometries considered. For clarity, only relevant Si surface atoms are indicated.

TABLE 1: Adsorption Energies, Dimer Length, and Dimer Angle for the Geometries Shown in Figure 1[a]

model	E_{ads} [eV]	d[b] [Å]	ω[c] [deg]
D	3.21 (3.07)	2.41	2.0 (2.4)
D′	2.64 (2.83)	2.34[d]	−1.7[d]
		2.43[e]	2.7[e]
P	0.34 (0.29)	2.39	8.6
P′	0.32 (0.27)	2.30	4.2
F	0.38	2.34	7.8
F′	1.92	2.39	1.3

[a] For comparison, DFT results from ref 6 are included in parentheses. [b] Dimer length, $d_{clean} = 2.35$ Å. [c] Dimer angle, $\omega_{clean} = 10.9°$. [d] Value for chlorine-terminated Si dimer. [e] Value for methyl-terminated Si dimer.

the adsorption of methyl chloride. In the following, we consider a coverage of one molecule adsorbed per $c(4 \times 2)$ surface unit cell.

Figure 1 shows schematically the energetically favored subset of Si(001)/CH_3Cl interface configurations studied here. The nomenclature is chosen to indicate the character of the adsorption: P and P′ denote physisorbed (or weakly adsorbed), D and D′ dissociated, and F and F′ fragmented configurations, where part of the molecule is ejected from the adsorption site. The clean surface will be referred to as "C" in the following.

The respective adsorption energies are given by

$$E_{ad} = E_{subs} + E_{ads} - E_{subs/ads} \quad (1)$$

where E_{subs}, E_{ads}, and $E_{subs/ads}$ are the total energies of the substrate, the adsorbate, and the substrate−adsorbate system, respectively. The calculated values are compiled in Table 1.

To obtain realistic estimates for the relative stabilities of the fragmented states F and F′, we assume that, after adsorption of methyl chloride, the remaining fragments are ejected into vacuum, reacting to form either Cl_2 or C_2H_6. Thus we obtain the following adsorption energies:

$$E_{ads}(F) = \left\{E(\mathrm{Si(001)}) + E(\mathrm{CH_3Cl}) - \frac{1}{2}E(\mathrm{Cl_2})\right\} - E(\mathrm{Si(001)CH_3}) = 0.38\ \mathrm{eV} \quad (2a)$$

$$E_{ads}(F') = \left\{E(\mathrm{Si(001)}) + E(\mathrm{CH_3Cl}) - \frac{1}{2}E(\mathrm{C_2H_6})\right\} - E(\mathrm{Si(001)Cl}) = 1.92\ \mathrm{eV} \quad (2b)$$

It is interesting to note that, assuming equilibrium of the surface with a Cl_2 or C_2H_6 reservoir, the adsorption of a single methyl group releases considerably less energy than the adsorption of chlorine. This is in agreement with the experimental observation of a Cl/CH_3 ratio on the surface of approximately 2:1 after heating the exposed sample to 150 °C.[4] Also in ref 4, a pronounced tendency for the formation of extended monochloride islands was found. That can be explained by the attractive interaction between adsorbed Cl atoms, which manifests itself in the considerable increase of the adsorption energy from 1.92 to 4.11 eV upon increasing the Cl coverage from 0.125 to 1 ML. Also the interaction between the methyl groups is attractive. We find a corresponding increase of the adsorption energy from 0.38 to 0.98 eV. Due to the temperature and pressure dependence of the respective chemical potentials, however, the relative stability of F and F′ will strongly depend on the preparation conditions. In fact, Brown and Ho[3] found no chlorine on the Si(001) surface for exposure temperatures ≥700 K.

Our findings concerning the adsorption geometries and adsorption energies agree very well with the results of Romero et al.,[6] as can be seen from Table 1. The agreement is particularly good for the data of ref 6 that were obtained using the Perdew-Burke-Ernzerhof (PBE) parametrization[19] of the exchange and correlation energy. Romero and co-workers calculate for the structure P, for instance, adsorption energies of 0.10 and 0.29 eV using the BLYP[20] and PBE parametrization of exchange and correlation, respectively. The latter value is very close to the 0.34 eV obtained in the present work using PW91. This is because PBE is essentially a reparametrization of PW91 and should therefore yield very similar adsorption energies. The deviation of the BLYP results may be attributed to the different composition of exchange (Becke[20]) and correlation (Lee, Yang, Parr[21]) parts in this functional.

In agreement with ref 6 as well as with the semiempirical calculations of Lee and Kim,[5] we find the dissociative adsorption of methyl chloride with CH_3 and Cl fragments bonded to the same dimer (structure D) to be the most favored among the investigated adsorption geometries, at least for the complete adsorption of one molecule, that is, neglecting the formation of, for example, monochloride dimers. Bonding of the methyl group and the chlorine to different Si dimers (structure D′) leads to an adsorption energy that is lower by 0.57 eV. However, as discussed by Romero et al.,[6] the activation energy to form structure D′ may be substantially lower than the one that needs to be overcome to form configuration D.

3.2. Electronic Structure. To quantify the charge transfer induced by the adsorption of methyl chloride, we calculate the spatially resolved charge density difference

$$\Delta\rho(\mathbf{r}) = \rho_{ads/subs}(\mathbf{r}) - \rho_{subs}(\mathbf{r}) - \rho_{ads}(\mathbf{r}) \quad (3)$$

where $\rho_{ads/subs}$, ρ_{subs}, and ρ_{ads} are the (negative) charge densities of the relaxed adsorbate−substrate system, of the clean relaxed surface, and of the adsorbate without substrate, respectively. From this quantity, the number of transferred electrons,

$$Q^{\pm} = \int_{\Delta\rho(\vec{\mathbf{r}})\gtrless 0} \mathrm{d}\mathbf{r}\ \Delta\rho(\mathbf{r}) \quad (4)$$

the length of the Q^+-Q^- dipole projected onto the surface normal,

$$d_z = \frac{1}{Q^+}\int_{\Delta\rho(\mathbf{r})>0} \mathrm{d}\mathbf{r}\ z\Delta\rho(\mathbf{r}) - \frac{1}{Q^-}\int_{\Delta\rho(\mathbf{r})<0} \mathrm{d}\mathbf{r}\ z\Delta\rho(\mathbf{r}) \quad (5)$$

and the z-component of the dipole, $p_z = |Q^{\pm}|d_z$, are derived. By averaging the charge density difference over the surface area,

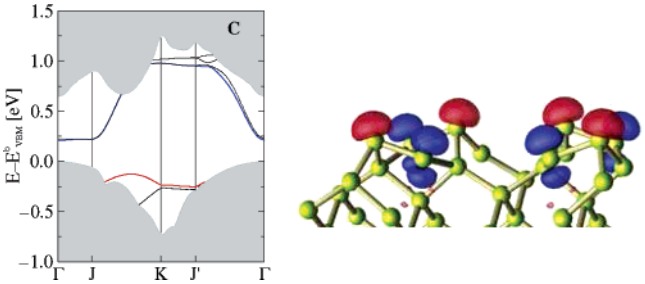

Figure 2. Clean surface C: (left) surface band structure; gray regions indicate the projected Si bulk band structure, red indicates D_{up} band, and blue indicates D_{down} band, and energies are given with respect to the bulk valence band maximum (VBM); (right) square moduli of the wave functions of HOMO (red) and LUMO (blue) at point *K*; isosurface value = 0.02 e/Å^3.

TABLE 2: Characteristics of Adsorbate−Substrate Charge Transfer (See Text)

model	$\|Q^{\pm}\|$	$\|Q^{\pm}_{\|\|}\|$	d_z [Å]	$d_{\|\|}$ [Å]	p_z [D]
D	3.46*e*	0.81*e*	−0.42	−1.78	−7.0
D′	7.02*e*	1.15*e*	0.18	1.06	5.9
P	2.39*e*	0.57*e*	0.10	0.43	1.2
P′	4.49*e*	1.85*e*	0.83	2.00	17.9
F	3.33*e*	1.49*e*	0.86	1.92	13.8
F′	4.01*e*	0.69*e*	0.13	0.75	0.5

we obtain the vertical charge redistribution

$$Q^{\pm}_{||} = \int_{\bar{\Delta\rho}(z)\gtrless 0} \mathrm{d}\mathbf{r}\, \bar{\Delta\rho}(z) \tag{6}$$

with

$$\bar{\Delta\rho}(z) = \frac{1}{A}\int_A \mathrm{d}x\, \mathrm{d}y\, \Delta\rho(\mathbf{r}) \tag{7}$$

The corresponding vertical charge separation length, $d_{||}$, is then given by eq 5 with $\Delta\rho(\mathbf{r})$ replaced by $\bar{\Delta\rho}(z)$. The calculated values are compiled in Table 2.

From these data, it is obvious that the charge transfer across the interface depends strongly on the details of the bonding, in contrast to the situation of simple adsorbates such as metals.[22] Models based solely on the difference in electronegativity between the molecule constituents and the substrate do not necessarily hold. Only the structure D shows a charge transfer from Si toward the molecule, as might be expected from the electronegativities of 2.55 (C), 2.20 (H), 3.16 (Cl), and 1.90 (Si). The structure D′, where Cl and CH_3 bond to different Si dimers, leads to a nominal charge transfer toward the substrate. The complexity of the charge transfer is due to the electronic properties of the dimerized Si(001) surface: An electric double layer is formed by filled and empty Si dimer atom dangling bonds.[22] Any changes of the dimer tilting will thus automatically result in a charge transfer along the surface normal.

Our calculated surface band structure of clean Si(001) $c(4 \times 2)$ is shown in Figure 2; it exhibits a semiconducting surface with an energy gap of about 0.3 eV, in accordance with previous density-functional calculations (e.g., see ref 23). The most important features in the bulk gap region are the D_{up} and D_{down} bands, corresponding to the "up" and "down" dimer contributions. There is nearly no energy dispersion perpendicular to the dimer rows but strong dispersion along *JK*.

Although models D and D′ seem to be comparable with respect to adsorption energy and geometry, their band structures are clearly different. This is to be expected, given the fact the structure D allows for completely occupying all surface bonds,

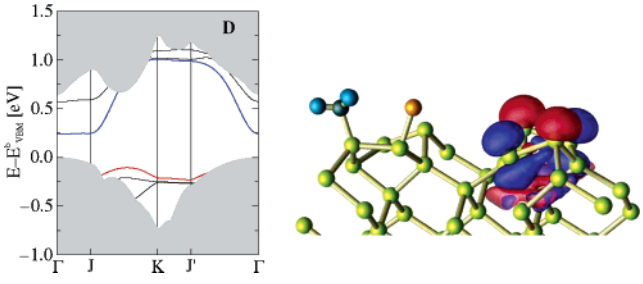

Figure 3. Configuration D: (left) surface band structure; gray regions indicate the projected Si bulk band structure; (right) character of HOMO (red) and LUMO (blue) at point *K*; isosurface value = 0.02 e/Å^3.

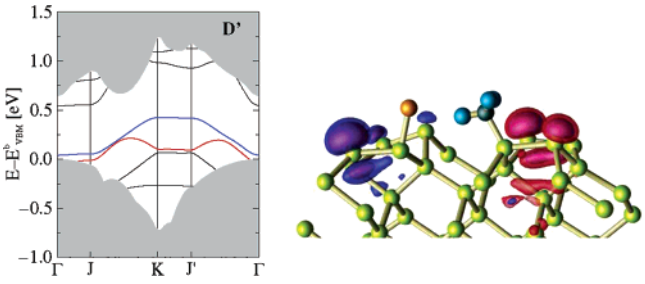

Figure 4. Configuration D′: (left) surface band structure; gray regions indicate the projected Si bulk band structure; (right) character of HOMO (red) and LUMO (blue) at point *K*; isosurface value = 0.02 e/Å^3.

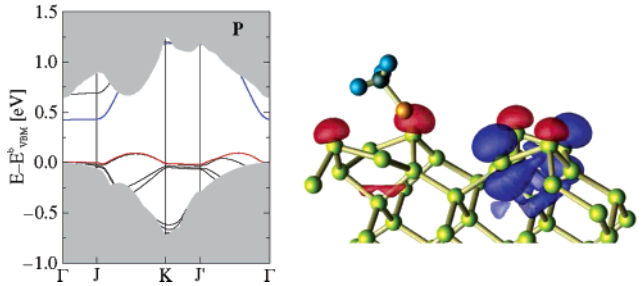

Figure 5. Configuration P: (left) surface band structure; gray regions indicate the projected Si bulk band structure; (right) character of HOMO (red) and LUMO (blue) at point *K*; isosurface value = 0.02 e/Å^3.

whereas D′ leaves unpaired electrons in Si dimer states. Accordingly, the band structure of D (Figure 3) is qualitatively similar to that of the clean surface; it remains semiconducting. However, the energetical degeneracy of the D_{down} bands is lifted upon adsorption. In case of the D′ model (Figure 4), the D_{up} band is shifted upward by 0.5 eV, the D_{down} band lowered by 0.5 eV, and the bands overlap and thus render the surface metallic. These electronic changes are also reflected in structural modifications of the Si surface dimers: The tilting of the chlorine-terminated (methyl-terminated) dimer is reduced to −1.7° (2.7°) compared to the clean surface. The energies of the Si dimer dangling bond states are thus very close and overlap due to the interaction. This also explains the result that D is energetically favored over D′. The isosurface plots of occupied and unoccupied surface states confirm the strong qualitative differences between D and D′. Whereas the orbital characters of these states for model D are similar to that of the clean surface, the corresponding wave functions in model D′ overlap after the formation of covalent bonds between Cl and C and "down" Si atoms. Note that in structure D′ the relative height of the Si atoms of the chlorine-terminated dimer is changed with respect to the clean surface, indicated by the minus sign of the tilting angle in Table 1. For consistency reasons in the discussion of the electronic structure, though, the nomenclature of "up" and "down" is maintained.

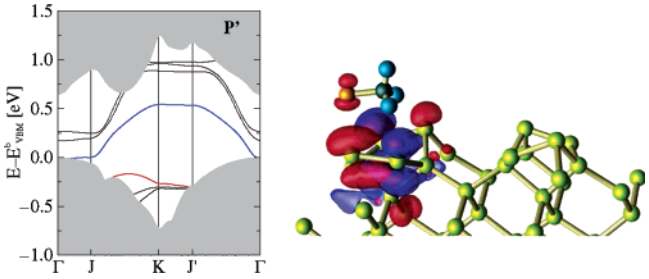

Figure 6. Configuration P′: (left) surface band structure; gray regions indicate the projected Si bulk band structure; (right) character of HOMO (red) and LUMO (blue) at point *K*; isosurface value = 0.02 e/Å^3.

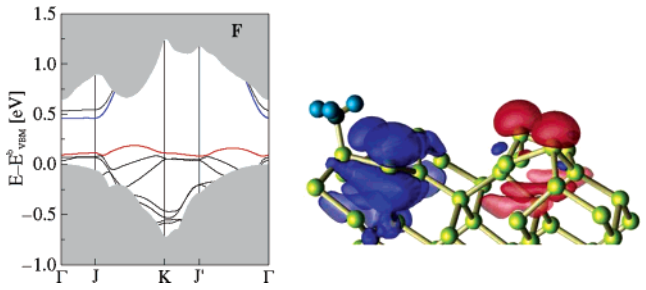

Figure 7. Configuration F: (left) surface band structure; gray regions indicate the projected Si bulk band structure; (right) character of HOMO (red) and SOMO (singly occupied molecular orbital, blue) at point *K*; isosurface value = 0.02 e/Å^3.

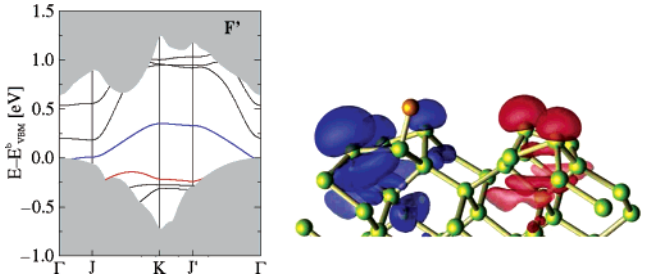

Figure 8. Configuration F′: (left) surface band structure; gray regions indicate the projected Si bulk band structure; (right) character of HOMO (red) and SOMO (blue) at point *K*; isosurface value = 0.02 e/Å^3.

The physisorbed states P and P′ (Figures 5 and 6) are both loosely bonded to the surface dimers but in a quite different way. In structure P, a weak bond between Cl and the "down" Si atom is formed, like in the geometries D, D′, F, and F′, whereas model P′ is the only configuration with Cl near the "up" Si atom. This difference manifests itself in the band structures: the Si surface bands for model P are shifted upward by roughly 0.5 eV; thus the occupied D_{up} band now completely lies in the energy region of the Si bulk gap, whereas the unoccupied surface bands are pushed toward the bulk conduction band minimum. In configuration P′, the energetic position of the D_{up}-like band remains unchanged with respect to the clean surface. The D_{down}-derived band is lowered and reaches the bulk valence band maximum; the surface thus becomes metallic. Its bandwidth is reduced to only 0.4 eV compared to 0.9 eV for the clean surface, resulting from the decrease of the dimer buckling, compare Table 1.

Consistent with the reduction of the Si dimer tilting to only 1.3°, the bandwidth of the D_{down}-derived band of structure F′ (Figure 8) is only 0.25 eV, thus even smaller than that for model P. The band structure of F (Figure 7), in contrast, is again very similar to the one of P: all bands are shifted upward by about 0.5 eV. In both models F and F′, the D_{down}-like band is occupied with one electron at *K*, again giving rise to a semimetallic surface after adsorption.

To account for the variation of the surface dipole layer upon adsorption of methyl chloride, we consider the microscopic electrostatic potential

$$V_C(\mathbf{r}) = V_{ps}^{loc}(\mathbf{r}) + V_H(\mathbf{r}) + V_{XC}(\mathbf{r}) \tag{8}$$

calculated within DFT-GGA.[24,25] V_{ps}^{loc}, V_H, and V_{XC} denote the local part of the pseudopotential, the Hartree potential, and the exchange−correlation potential, respectively. The averaged and smoothed electrostatic potential in the [001] direction is given by

$$\overline{V_C}(z) = \frac{1}{L}\int_{z-L/2}^{z+L/2} dz' \frac{1}{A}\int_A dx\, dy\, V_C(x,y,z') \tag{9}$$

where *A* corresponds to the area of the surface unit cell and *L* to the distance between the substrate layers. The differences $\Delta\overline{V_C}(z)$ between the Si(001)/CH_3Cl interfaces and the clean relaxed Si(001)$c(4 \times 2)$ surface are shown in Figure 9.

The results show that the changes of the surface dipole, corresponding to the changes of the ionization energy, cannot directly be related to the (vertical) charge transfer. For example, structures D and D′ lead to a vertical charge transfer along and opposite to the direction of the surface normal. Similar observations were recently made for the adsorption of cesium on GaAs[26] and for uracil-covered Si(001) surfaces.[27] Nevertheless, in both cases the ionization energy is (marginally) increased compared to the clean Si surface. It can be seen that models P and P′ lead to a reduction of the surface dipole potential by about 0.70 and 0.30 eV, respectively, so the ionization energies of the adsorbed surfaces are also lowered by the same amount. The relatively large value of 0.70 eV in the physisorbed configuration P may be attributed to the interplay between the (still quite prominent)

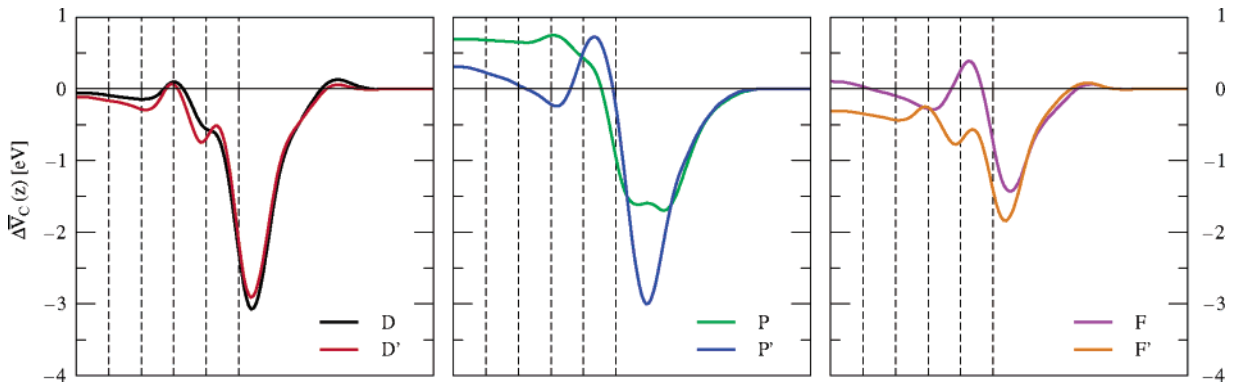

Figure 9. Difference of the averaged and smoothed electrostatic potentials of Si(001)/CH_3Cl adsorption configurations and the clean Si(001) $c(4 \times 2)$ surface plotted along the surface normal in the interface region. Dashed lines indicate the positions of the Si layers.

electric dipole layer of the surface and the effective vertical dipole moment due to charge transfer from molecule to surface. For comparison, clean Si(001) surfaces experience a reduction of the ionization energy by about 0.35 eV upon exposure to atomic hydrogen.[22] The difference potentials for the fragmented structures F and F′ are, despite an overall comparable line shape, strikingly different. Whereas adsorption of a methyl group on a Si dimer results in a small decrease of the surface dipole by 0.10 eV, the formation of a strong covalent Si−Cl bond is sufficient to increase the surface dipole by 0.30 eV. The changes of the ionization energy for the configurations in which the Si(001) surface is completely passivated by a full monolayer of methyl groups or chlorine atoms are even more drastic: For the monochloride Si surface, we find an increase of the ionization energy with respect to the clean surface of 1.04 eV, in good agreement with a previous theoretical result of 1.09 eV obtained by Krüger and Pollmann.[28] For the Si surface covered with a monolayer of methyl groups, we predict a strong decrease of the ionization energy by 1.88 eV. The major part of this reduction is attributed to the dipole layer formed between the plane of the hydrogen atoms (charge depletion) and the plane of the carbon atoms (charge accumulation).

4. Summary

The adsorption of methyl chloride on Si(001) was investigated is studied using first-principles calculations. Concerning the adsorption geometries, we find a strong tendency for molecular dissociation and fragmentation. The charge-transfer processes have been characterized by the number of transferred electrons and the net dipole moment. Additionally, the surface dipole layer variations have been discussed with respect to the different bonding characteristics. The electronic band structures revealed a remarkable influence of the adsorption geometries on the surface states.

Acknowledgment. Grants of computer time from the Leibniz-Rechenzentrum München and the Höchstleistungsrechenzentrum Stuttgart are gratefully acknowledged. We thank the Deutsche Forschungsgemeinschaft for financial support (Grant SCHM-1361/6).

References and Notes

(1) Dabrowski, J.; Müssig, H.-J. *Silicon Surfaces and Formation of Interfaces;* World Scientific: Singapore, 2000.

(2) Bent, S. F. *Surf. Sci.* **2002**, *500*, 879.

(3) Brown, K. A.; Ho, W. *Surf. Sci.* **1995**, *338*, 111.

(4) Bronikowski, M. J.; Hamers, R. J. *J. Vac. Sci. Technol., A* **1995**, *13*, 777.

(5) Lee, J. Y.; Kim, S. *Surf. Sci.* **2001**, *482*, 196.

(6) Romero, A. H.; Sbraccia, C.; Silvestrelli, P. L.; Ancilotto, F. *J. Chem. Phys.* **2003**, *119*, 1085.

(7) Kresse, G.; Furthmüller, J. *Comput. Mater. Sci.* **1996**, *6*, 15.

(8) Perdew, J. P.; Chevary, J. A.; Vosko, S. H.; Jackson, K. A.; Pederson, M. R.; Singh, D. J.; Fiolhais, C. *Phys. Rev. B* **1992**, *46*, 6671.

(9) Hamprecht, F. A.; Cohen, A. J.; Tozer, D. J.; Handy, N. C. *J. Chem. Phys.* **1998**, *109*, 6264. Adamo, C.; Barone, V. *J. Chem. Phys.* **1999**, *110*, 6158. Boese, A. D.; Doltsinis, N. L.; Handy, N. C.; Sprik, M. *J. Chem. Phys.* **2000**, *112*, 1670. Becke, A. D. *J. Comput. Chem.* **1999**, *20*, 63.

(10) Benco, L.; Hafner, J.; Hutschka, F.; Toulhoat, H. *J. Phys. Chem. B* **2003**, *107*, 9756.

(11) Kganyago, K. R.; Ngoepe, P. E. *Mol. Simul.* **1999**, *22*, 39.

(12) Furthmüller, J.; Käckell, P.; Bechstedt, F.; Kresse, G. *Phys. Rev. B* **2000**, *61*, 4576.

(13) Preuss, M.; Schmidt, W. G.; Seino, K.; Furthmüller, J.; Bechstedt, F. *J. Comput. Chem.* **2004**, *25*, 112.

(14) Seino, K.; Schmidt, W. G.; Furthmüller, J.; Bechstedt, F. *Phys. Rev. B* **2002**, *66*, 235323.

(15) Seino, K.; Schmidt, W. G.; Preuss, M.; Bechstedt, F. *J. Phys. Chem. B* **2003**, *107*, 5031.

(16) Pulay, P. *Chem. Phys. Lett.* **1980**, *73*, 393.

(17) Wood, D. M.; Zunger, A. *J. Phys. A* **1985**, *18*, 1343.

(18) Krüger, P.; Pollmann, J. *Phys. Rev. Lett.* **1995**, *74*, 1155.

(19) Perdew, J. P.; Burke, K.; Ernzerhof, M. *Phys. Rev. Lett.* **1996**, *77*, 3865.

(20) Becke, A. D. *Phys. Rev. A* **1988**, *38*, 3098.

(21) Lee, C.; Yang, W.; Parr, R. C. *Phys. Rev. B* **1988**, *37*, 785.

(22) Mönch, W. *Semiconductor Surfaces and Interfaces*, 3rd ed.; Springer-Verlag: Berlin, Heidelberg; 2001.

(23) Ramstad, A.; Brocks, G.; Kelly, P. J. *Phys. Rev. B* **1995**, *51*, 14504.

(24) Schlüter, M.; Chelikowsky, J. R.; Louie, S. G.; Cohen, M. L. *Phys. Rev. B* **1975**, *12*, 4200.

(25) Schmidt, W. G.; Bechstedt, F.; Srivastava, G. P. *Surf. Sci. Rep.* **1996**, *25*, 141.

(26) Hogan, C.; Paget, D.; Garreau, Y.; Sauvage, M.; Onida, G.; Reining, L.; Chiaradia, P.; Corradini, V. *Phys. Rev. B* **2003**, *68*, 205313.

(27) Seino, K.; Schmidt, W. G.; Bechstedt, F. *Phys. Rev. B*, accepted for publication.

(28) Krüger, P.; Pollmann, J. *Phys. Rev. B* **1993**, *47*, 1898; private communication.